BIOCHEMICAL PHARMACOLOGY 76 (2008) 805–815

available at www.sciencedirect.com

ScienceDirect

journal homepage: www.elsevier.com/locate/biochempharm

A common "hot spot" confers hERG blockade activity to α-scorpion toxins affecting K^+ channels

Yousra Abdel-Mottaleb [a], *Gerardo Corzo* [b], *Marie-France Martin-Eauclaire* [c], *Honoo Satake* [d], *Brigitte Céard* [c], *Steve Peigneur* [a], *Praveen Nambaru* [a], *Pierre-Edouard Bougis* [c], *Lourival D. Possani* [b], *Jan Tytgat* [a,*]

[a] *Laboratory of Toxicology, University of Leuven, O&N 2, Herestraat 49, P.O. Box 922, 3000 Leuven, Belgium*
[b] *Departamento de Medicina Molecular y Bioprocesos, Instituto de Biotecnología, Universidad Nacional Autónoma de México, UNAM. Apartado Postal 510-3, Cuernavaca Morelos 61500, Mexico*
[c] *Université de la Méditerranée, BIMC, CNRS FRE 2738, Faculté de Médecine Nord, 51, Bd Pierre Dramard, F-13916 Marseille Cedex 20, France*
[d] *Suntory Institute for Bioorganic Research, 1-1-1 Wakayamadai, Shimamoto-Cho, Mishima-Gun, Osaka 618-8503, Japan*

ARTICLE INFO

Article history:
Received 25 March 2008
Accepted 2 July 2008

Keywords:
hERG channels
Scorpion toxins
K^+ channels
α-KTx
γ-KTxs

ABSTRACT

While α-KTx peptides are generally known for their modulation of the *Shaker*-type and the Ca^{2+}-activated potassium channels, γ-KTxs are associated with hERG channels modulation. An exception to the rule is BmTx3 which belongs to subfamily α-KTx15 and can block hERG channels. To explain the peculiar behavior of BmTx3, a tentative "hot spot" formed of 2 basic residues (R18 and K19) was suggested but never further studied [Huys I, et al. BmTx3, a scorpion toxin with two putative functional faces separately active on A-type K^+ and HERG currents. Biochem J 2004;378:745–52].

In this work, we investigated if the "hot spot" is a commonality in subfamily α-KTx15 by testing the effect of (AmmTx3, Aa1, discrepin). Furthermore, single mutations altering the "hot spot" in discrepin, have introduced for the very first time a hERG blocking activity to a previously non-active α-KTx.

Additionally, we could extend our results to other α-KTx subfamily members belonging to α-KTx1, 4 and 6, therefore, the "hot spot" represents a common pharmacophore serving as a predictive tool for yet to be discovered α-KTxs.

1. Introduction

The human ether-à-go-go related gene (hERG) encodes the pore-forming subunit of the rapid delayed rectifier K channels (I_{Kr}) expressed in cardiac myocytes [2,3]. The keen interest in the role of hERG channels in the heart stems from hERG being the gene product involved in chromosome 7-associated long QT syndrome (LQTS) [4] and from the fact that the blockade of hERG by a wide range of prescription medications causes LQTS, which is the commonest cause of drug-induced cardiac arrhythmia and sudden death [5]. In addition to the heart, hERG channels are also expressed in a range of tissues including neurons [6], neuroendocrine glands [7,8] smooth muscle [9] and are involved in cancer cell growth [10]. There has been a strong interest in the structure–function relationship of the hERG channel, fueled by the need of pharmaceutical industry to predict chemical structures that may lead to

* *Corresponding author*. Fax: +32 16 3234 05.
E-mail address: jan.tytgat@pharm.kuleuven.be (J. Tytgat).
0006-2952/$ – see front matter
doi:10.1016/j.bcp.2008.07.008

hERG/I_{Kr} suppression, which can be potentially linked to the acquired LQTS [11].

Peptide toxins are valuable components in the defense and prey capture of venomous animals such as scorpions. Scorpion toxins affecting K^+ channels (KTxs) have been divided into 4 large families: α-, β-, γ-, and κ-KTxs based on the classification proposed by Tytgat et al. [12]. Many studies have tackled the interaction between toxins and the surface of the channels. At least 4 models of interaction between KTxs and K^+ channels have been proposed (for a review, see [13,14]). Most of those models attempted to explain the interaction between α-KTxs and voltage-gated K channels, such as the dyad model [15], or Ca^{2+}-activated K^+ channels, such as the basic ring model [16]. As for the interaction between γ-KTxs and hERG channels, the 2 heads model has been proposed [17]. However, each of the models has its applications and its limitations, therefore, novel models which can overcome those limitations remain to be elucidated and the molecular mechanisms underlying those models identified. Recently, the interaction between a chimeric K^+ channel KcsA-Kv1.3 and a member of α-KTx family have been solved using high-resolution solid-state NMR spectroscopy. Significant structural rearrangements in different segments of the ligand and the ligand-binding site of the channel were seen, including the selectivity filter. As a result, the filter collapses shut [18]. KTxs have been essential tools for the first purifications, structural analysis, localization and identification of the pore-forming regions of K^+ channels [19–21], hence, toxins targeting the hERG channel are useful tools in this line of research [22]. Several peptides affecting hERG channels have been identified [1,23–26]. Except for BmTx3 from *Mesobuthus martensii*, which belongs to α-KTx [1], most hERG channel toxins belong to γ-KTxs [13]. Nevertheless, they all adopt a highly conserved secondary structure, the cysteine-stabilized α/β scaffold. While α-KTxs interact with channels through their β-sheets, γ-KTxs modulate hERG through their α-helix. BeKm-1 from *Mesobuthus eupeus* is one of the best studied cases of peptide toxins belonging to γ-KTxs [25,27]. BeKm-1 binds to hERG's outer vestibule to suppress ion conduction through the pore. An alanine scanning mutagenesis study showed that BeKm-1 uses its α-helix and the following turn as the interaction surface in binding to the hERG channel and pointed out to several residues, among which 2 basic residues, Lys18 and Arg20 [28]. When BmTx3 was found to block hERG channels, the effect was assigned to the same "hot spot": 2 basic residues [1] on the α-helix side of the peptide in accordance with BeKm-1 [1]. BmTx3 was therefore proposed to dispose of 2 functional faces, a typical dyad through which it blocks A^+-type currents on the β-sheet side and the 2 basic residues (Arg18 and Lys19) on the α-helix side of the peptide that blocks the hERG current.

In the present work, we have investigated the hERG blocking activity of AmmTx3 from the Moroccan scorpion *Androctonus mauretanicus mauretanicus* [29–31] which is a natural mutant of BmTx3 (91% similarity), as well as other members of subfamily α-KTx15 such as Aa1 from *Androctonus australis* [32] with 89% similarity and discrepin from *Tityus discrepans* with 51% similarity [33,34]. The credibility of the proposed "hot spot" has been proven using 8 mutants of AmmTx3 and discrepin and was extended to other selected toxins belonging to subfamilies α-KTx1, 4 and 6.

2. Methods

2.1. Toxins preparations

2.1.1. Construction of the synthetic AmmTx3 gene and mutants

All oligonucleotides used herein were from MWG Biotech (Germany). Four overlapping oligonucleotides (primers I, II, III, and IV) were optimised for bacterial expression and designed according to the amino acid sequence of native AmmTx3 [29]. Primer I (63 mers 5′-GGG**GGTACC**CGGTGGCGGTGGCTCTG-GCGGTGGCGGTATGCAGATTGAAACCAACAAGAAGTG-3′) and primer II (59 mers 5′-GCAGATTGAAACCAACAAGAAGTGCC-AGGGCGGCAGCTGCGCGAGCGTGTGCCGCAAAG-3′) were forward, and primer III (55 mers 5′-CCATTGATGCATTTCCCC-GCCGCCACGCCGATCACTTTGCGGCACACGCTCGCGC-3′) and primer IV (55 mers 5′-CGGGATCC**AAGCTT**ACGGGTAGCA-CACGCAGCGGCCATTGATGCATTTCCCCGCC-3′) were reverse. Sequences corresponding to linkers are underlined and the two restriction sites Kpn I and Hind III are in bold. The Met codon introduced as a chemical cleavage site in order to recover the free recombinant toxin from the fused ZZ protein is underlined twice.

The polymerase chain reaction (PCR) strategy performed to build the synthetic AmmTx3 gene was the following: in a reaction volume of 50 μl primers II and III (1 pmol) corresponding to the internal sequence of the AmmTx3 were added in a ratio of 1/100 to primers I and IV (100 pmol) corresponding to the N- and C-terminal sequences of the toxin. The PCR reaction steps consisted in an initial denaturation (94 °C, 2 min), followed by 25 cycles of denaturation (94 °C, 1 min), annealing (55 °C, 2 min) and elongation (72 °C, 3 min), and a final elongation (72 °C, 10 min). We used 1 μl PWO DNA polymerase [35] in the experimental conditions recommended by the manufacturer. The final AmmTx3 synthetic gene construct was purified on a 3% Nusieve agarose gel (FMC bioproduct, Rockland, Maine, USA) and has the following sequence:

GGGGGTACCCGGTGGCGGTGGCTCTGGCGGTGGCGGTATG CAG ATT GAA ACC AAC AAG AAG TGC CAG GGC GGC AGC TGC GCG AGC GTG TGC CGC AAA GTG ATC GGC GTG GCG GCG GGG AAA TGC ATC AAT GGC CGC TGC GTG TGC TAC CCG TAA GCTTGGATCCCG.

AmmTx3 and mutants were all expressed in *E. coli* as a fusion protein with the ZZ domain, a synthetic IgG-binding domain of protein A [36], using the vector pEZZ18 (Pharmacia GE Healthcare, Fairfuld, CT, USA). The above AmmTx3 gene construct was digested with Kpn I and Hind III (New England Biolabs Inc., USA) according to the manufacturer's instructions to be inserted in the vector, subsequently named pEZZ/AmmTx3.

Mutants were derived from the above AmmTx3 synthetic gene according to the megaprimer method [37]. Briefly, 1.9 ng of pEZZ/AmmTx3 was taken as template for a first PCR (94 °C, 2 min, followed by 30 cycles at 94 °C, 1 min, 55 °C, 1 min 30 s, 72 °C, 2 min and a final elongation step at 72 °C, 7 min). The forward primers (50 pmol) were the following: mutant K6V 5′-GAAACCAACGTGAAGTGCCAGGG-3′, mutantR18A 5′-CGAGC-GTGTGCGCCAAAGTGATC-3′, and mutant K19A 5′-GTGTGCC-GCGCAGTGATCGGC-3′, and the unique reverse primer

(50 pmol) was 5′-GAACGTGGCGAGAAAGGAAGGGAAGAAAG-3′. The three different fragments (megaprimers) obtained were purified on Seaplaque FMC 1.25% agarose and individually used (500 ng) for a second PCR. First an elongation was performed (3 cycles, 96 °C, 3 min, 62 °C, 2 min, 66 °C, 2 min, and 65 °C, 6 min), followed by a digestion with 0.5 μl by DpnI (New England Biolabs) for 90 min, and, secondly, 1 μl PWO polymerase, 20 pmol of the same reverse primer 5′-GAACGTGGCGAGAAAGGAAGGGAAGAAAG-3′ and 20 pmol of the forward primer 5′-GGTGTAGGTATTGCATCTGTAACTT-TAGG-3′ were added, followed by 25 cycles (96 °C, 1 min, 58 °C, 30 s, 72 °C 2 min), and a final elongation step at 72 °C, 7 min. The PCR products were then purified by Qiaquick purification kit (Qiagen N.V., the Netherlands), digested with Kpn I and Hind III, and ligated into pEZZ18 (Pharmacia GE Healthcare, Fairfuld, CT, USA). All clones were proofreading sequenced (Cogenics Genome express SA, Mylan, France).

2.1.2. *Expression, purification and N-terminal cyclization of the AmmTx3 and mutants*

pEZZ/AmTx3 encoding the ZZ/AmmTx3 fusion protein or mutants were transfected into HB 101 bacteria. Cells were grown for 20 h in one liter of TB culture medium supplemented with 100 μg/ml of ampicilline. The culture medium was centrifuged and the supernatant was load on an IgG-Sepharose column (Pharmacia GE Healthcare, Fairfuld, CT, USA). After purification of the fusion protein by affinity chromatography steps, recombinant toxins were subsequently kept free from the ZZ fragment by a chemical cleavage using 90 mM CNBr for 24 h at 37 °C in 0.1N HCl [38]. The mixture was then HPLC purified on a C18 reverse-phase column (Merck Ultrasphere 5 μm) as previously described [29]. At the end, about 2 mg of recombinant AmmTX3 and 1 mg of each mutant were produced from one litre of culture medium.

2.1.3. *N-terminal cyclization*

To further cyclize the N-terminal glutamine of the recombinant toxins into a pyroglutamic acid (Z), 5% (vol/vol) acetic acid was added to the non-cyclized toxins [39]. Incubation was performed at 37 °C during 24 h. The cyclization process was monitored both on HPLC and on Ultraflex MALDI-TOF (Bruker, Germany).

2.1.4. *Synthesis of discrepin and mutants*

Synthetic discrepin and 5 mutants with the following substitutions: V6K, I19R, D20K, [I19R, D20K] and [I19R, D20K, R21V] were prepared. The chemical synthesis was performed by solid-phase using fluoren-9-ylmethoxycarbonyl (Fmoc) methodology on an Applied Biosystems 433A peptide synthesizer. Fmoc-Pro-TrtA-PEG resin (Watanabe Chemical Industries, Ltd., Hiroshima, Japan) and pyroglutamic acid (Peptide Institute Inc., Osaka, Japan) were used to produce the adequate C- and N-terminal residues of the protein, respectively. Cleavage and deprotection of peptide from the resin were performed using a chemical mixture composed of 1g crystalline phenol, 0.2 g imidazole, 1 ml thioanisol, 0.5 ml 1,2-ethanedithiol in 20 ml TFA [40]. The resin was removed by filtration, and the deprotected peptides in solution were precipitated using cold ethyl ether. The precipitated peptides were washed twice with cold ether to remove remaining scavengers and protecting groups. The crude linear synthetic peptides were dried under a flow of nitrogen and dissolved in 20% aqueous acetonitrile.

2.1.5. *Purification of synthetic discrepin and mutants*

The crude linear synthetic peptides were purified by RP-HPLC (Waters 600, with dual wavelength detector model 2847, Milford, MA, USA) on a semi-preparative C_{18} column (5C18MS, 10 mm × 250 mm, Nacalai Tesque, Japan) to 90–95% homogeneity, in order to eliminate synthetic byproducts and incorrectly assembled peptides using a 60 min linear gradient from 0 to 60% aqueous acetonitrile/0.1% TFA (2 ml/min). The six-free cysteine residues were allowed to oxidize in air for 24 h at room temperature in a 0.2 M aqueous Tris-base solution containing 1 mM reduced glutathione/0.1 mM oxidized glutathione at pH 8.0. The folded synthetic toxins were purified by same RP-HPLC system mentioned on an analytical C_{18} column (5C18MS, 4.6 mm × 250 mm, Nacalai Tesque, Japan) using a 20 min linear gradient from 10 to 30% aqueous acetonitrile/0.1% TFA (1 ml/min).

The mass identity between the synthetic discrepin and the mutant peptides were verified by electro spray ionization mass spectrometry using a Finnigan LCQ^{DUO} ion trap mass spectrometer (San Jose, CA, USA).

2.1.6. *Circular dichroism (CD) measurements*

CD spectra were obtained on a Jasco J-725 spectropolarimeter (Jasco, Japan). The spectra were measured from 260 to 200 nm in 60% trifluoroethanol to promote hydrogen-bonding [41,42], pH 7.1 at room temperature, with a 1 mm path-length cell. Data were collected at 1 nm with a scan rate of 50 nm/min and a time constant of 1 s. The concentration of the peptides was 200 μg/ml. Data were the average of two separate recordings.

2.2. *Oocyte preparations*

The *in vitro* synthesis of cRNA encoding for hERG channels and injection of *Xenopus leavis* oocytes have been performed as previously described [1].

2.3. *Electrophysiological experiments*

Two-electrode voltage-clamp recordings were performed as previously described [1]. Statistical analysis between groups of data was carried out using the Student's *t*-test and a probability of <0.05 was considered to be statistically significant.

3. Results

3.1. *Preparation of toxins and mutants*

3.1.1. *Expression of AmmTx3 and mutants*

Three basic residues (K6V, R18A and K19A) supposed to be involved in the bioactivity of AmmTx3 on hERG channels were mutated. The mutation K6V was chosen according to the BmTx3 sequence [1]. AmmTx3 and mutants were all expressed as fusion protein in *E. coli* and purified from the culture medium by affinity chromatography. Homogeneity and validity of the

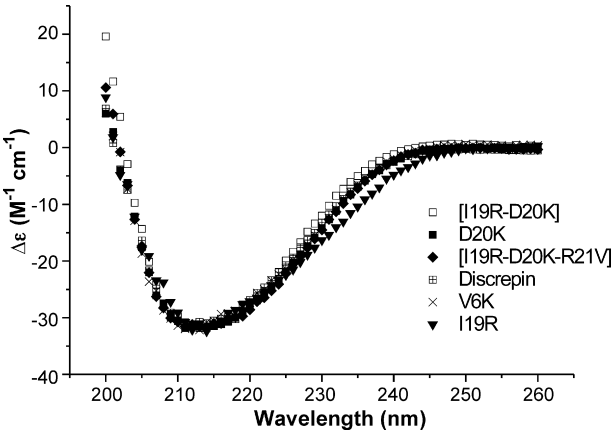

Fig. 1 – CD spectra of 200 μg/ml discrepin and discrepin mutants.

fusion protein was controlled using mass spectrometry. The amount of pure fusion protein obtained was 21 mg/l for the wild type toxin and the mutant K6V and 13 mg/l for the mutants R18A and K19A. At the end, about 2 mg of recombinant AmmTx3 and 1 mg of each mutant were recovered from 1 l of culture medium after cleavage by BrCN and HPLC purification. This is about 50% of the amount first expected from the fusion protein cleavage.

The expected theoretical monoisotopic masses of the toxin AmmTx3 and its mutants were: AmmTx3, 3819.8 Da; AmmTx3K6V, 3791.8 Da; AmmTx3R18A, 3735.7 Da; AmmTx3K19A 3763.7 Da. The experimental monoisotopic masses obtained were: AmmTX3, 3819.9; AmmTx3K6V, 3792.2; AmmTx3R18A, 3735.9; AmmTx3K19A, 3764 certifying the quality of the recombinant toxins obtained.

3.1.2. *Chemical synthesis of discrepin and mutants*

The overall assembly and cleavage yields of synthetic discrepin mutants were from 50 to 54% according to theoretical values of the peptidyl resin and the calculated mass increase for 0.1 mmol peptide to give around 250 mg of crude synthetic peptide. The final yields after chromatographic purification of the linear peptide and refolding for the discrepin mutants were 12, 8, 10, 6, and 5% for V6K, I19R, D20K, [I19R, D20K], and [I19R, D20K, R21V] respectively [43]. All chemically synthesized discrepin mutants were proven to coincide with the expected molecular masses; for instance, the experimental found versus the theoretical masses expected were 4177.0/4176.7 for the native, 4220.2/4219.9 for I19R, and 4190.4/4190.0 a.m.u. for D20K, respectively.

3.1.3. *Circular dichroism measurements*

The secondary structure of discrepin and discrepin mutants was measured by CD and analyzed using a neural network of 33 CD spectra of the proteins in the range 260–200 nm at 1 nm intervals. All peptides showed a minimum at 214–216 nm indicating a high content in β-sheets similar to the secondary structure of most known K^+ channel scorpion toxins such as Charybdotoxin [44] and Tc1 [45]. The CD data indicate that they are most likely to adopt a similar folding pattern (Fig. 1).

3.2. *Electrophysiological studies*

3.2.1. *Effect of AmmTx3 on hERG channels*

The common ''hot spot'' proposed to affect hERG is shown in Fig. 2. Fig. 3 illustrates the block induced by AmmTx3 on hERG channels. AmmTx3 (8 μM) reversibly blocked the small outward currents (I_t), the large outward tail currents (I_{tail}) and the inward currents ($I_{fully\ activated}$) in accordance with the data published on BmTx3 [1]. To measure the voltage-dependence of the channel activation, the activation curve was constructed using the normalized peak amplitudes of the I_{tail} values. The curve was then fitted using a simple Boltzman function, where $V_{1/2}$ is the half-maximal potential and S is the slope factor. No shift in the $V_{1/2}$ has been observed with the inhibition of the hERG currents upon addition of AmmTx3. The values of $V_{1/2}$ were -17.3 ± 0.6 and -17.6 ± 0.7 mV for the control condition and in case of the addition of the toxin respectively. And the slope factor was 8.1 ± 0.2 and 8 ± 0.3 mV respectively ($n = 4$).

The current–voltage (I_t–V_t) relationship of the test pulses is bell-shaped both in control and in the presence of AmmTx3. Its values have been normalized to $I_{fully\ activated}$, taking each oocyte as its own control. The results indicate that both the activation and inactivation processes increase with depolarization and are unaffected by the presence of the toxin. Further analysis of hERG channels recovery and deactivation were performed in control and in the presence of AmmTx3

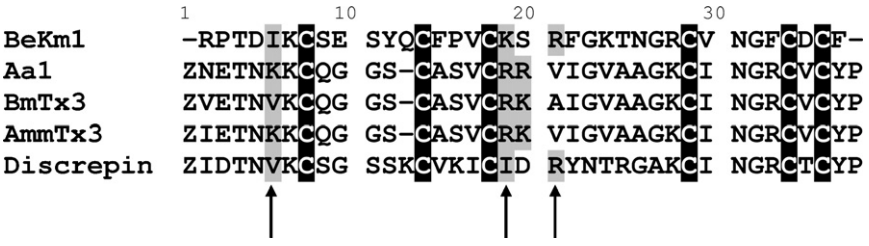

Fig. 2 – Alignment of the members of subfamily α-KTx15 based on the cysteine residues. The important residues involved in the proposed hERG ''hot spot'' are highlighted in grey namely 2 positive residues a Lys or Arg after the 3rd cysteine. The basic residue located before the 1st cysteine can also have an important effect. The alignment has been made using Bioedit program [46]. Toxin sequences references are databank accession numbers (either SwissProt, TREMBEL or GenBank) as retrieved from www.ncbi.nih.gov/entrez or from literature references: Q9BKB7, P60233, Q8I0L5, P60208, P84777 respectively.

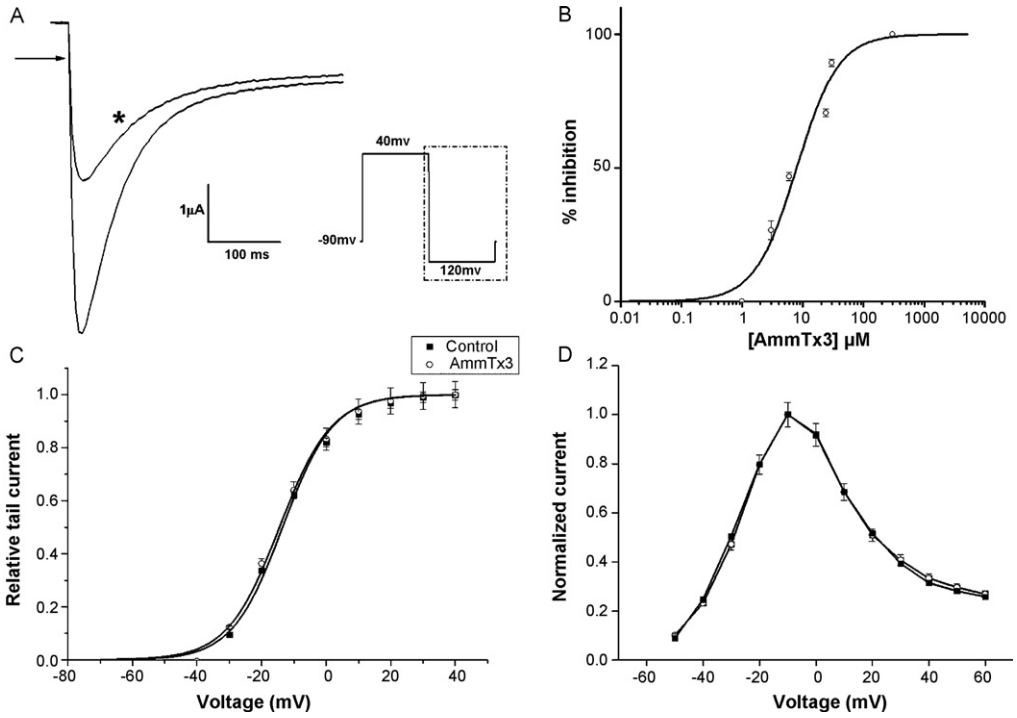

Fig. 3 – The effect of AmmTx3 on hERG channels. *Panel A*: tail current trace of hERG channels which were elicited by applying a +40 mV prepulse for 2 s followed by a step to −120 mV for 2 s where $I_{\text{fully activated}}$ is seen. A block of 50% was induced upon the addition of 8 μM AmmTx3 marked by the asterisk. *Panel B*: The normalized dose–response curve was plotted using the amplitude of the tail current as a function of increasing concentrations of AmmTx3. AmmTx3 could block hERG channels with an IC_{50} of 7.9 ± 1.4 μM and a Hill coefficient of 1.2 ± 0.2 (n = 5). *Panel C*: Activation curves of hERG channels in control conditions and in the presence of AmmTx3. *Panel D*: Current–voltage relationship in control conditions and in the presence of AmmTx3.

at $I_{\text{fully activated}}$. The tail currents rising and decaying were best fitted by a single exponential function where τ is the time constant. τ values were 1.56 ± 0.5 and 42.8 ± 4.3 ms for the 2 phases at control conditions which were not statistically significantly different from the values upon addition of AmmTx3 1.87 ± 0.4 and 40.1 ± 4.6 ms (n = 6).

The concentration-dependent inhibition of hERG currents by AmmTx3 is illustrated in the dose–response curve. hERG currents were fully activated by stepping to +40 mV from a holding potential of −90 mV. After each step, the voltage was returned to −120 mV and large inward tail currents could be recorded as previously described [25]. We have chosen to test the block on the fully activated currents at −120 mV since there have been no shift in the activation curves or in the IV curves. Furthermore, large amplitudes upon repolarization allow a good quantitative analysis of block in contrast to depolarization voltages during which hERG channels inactivate quickly, a situation not facilitating quantitative interpretation. The normalized dose–response curve was plotted using the amplitude of the tail current as a function of increasing concentrations of AmmTx3. AmmTx3 could block hERG channels with an IC50 of 7.9 ± 1.4 μM and a Hill coefficient of 1.2 ± 0.2 (n = 5). Since the IC_{50} value of AmmTx3 was almost 4 folds larger than that reported for BmTx3 [1], we investigated the possible reason behind it and constructed a mutant AmmTx3 K6V. The IC_{50} value of AmmTx3 K6V was found to be very close to that of BmTx3 (3.2 ± 0.75 μM, n = 8), confirming the role of K6V in AmmTx3.

Next we tested whether the same ''hot spot'' in BmTx3 is responsible for the inhibition of hERG channels by AmmTx3; we constructed 2 other mutants R18A and K19A, where in each case one of the 2 positive residues has been replaced by alanine. By testing on hERG channels, these mutants abolished the hERG blocking activity (n = 6) (Fig. 4).

3.2.2. *Effect of other α-Ktx 15 members*

Furthermore, we investigated other members of α-KTx 15 subfamily which either have the proposed ''hot spot'', such as Aa1, or do not dispose of the ''hot spot'' such as discrepin (Fig. 2). Due to the limited availability of Aa1 toxin we could only test it at one concentration: 600 nM which could induce a block of 25 ± 2.4% (n = 3, data not shown). In accordance with the proposed theory, discrepin possessing only 1 positive residue Arg at position 21, failed to induce any effects on hERG currents.

3.2.3. *Discrepin mutants*

To investigate whether the addition of 2 basic residues after the 3rd cysteine could confer a hERG blocking activity to the non-active discrepin, 4 mutants where constructed: I19R, D20K, a double mutant [I19R, D20K] and finally a triple mutant [I19R, D20K and R21V]. The discrepin mutants I19R and D20K could induce a block of 18.5 ± 3%, 20.2 ± 2.1%

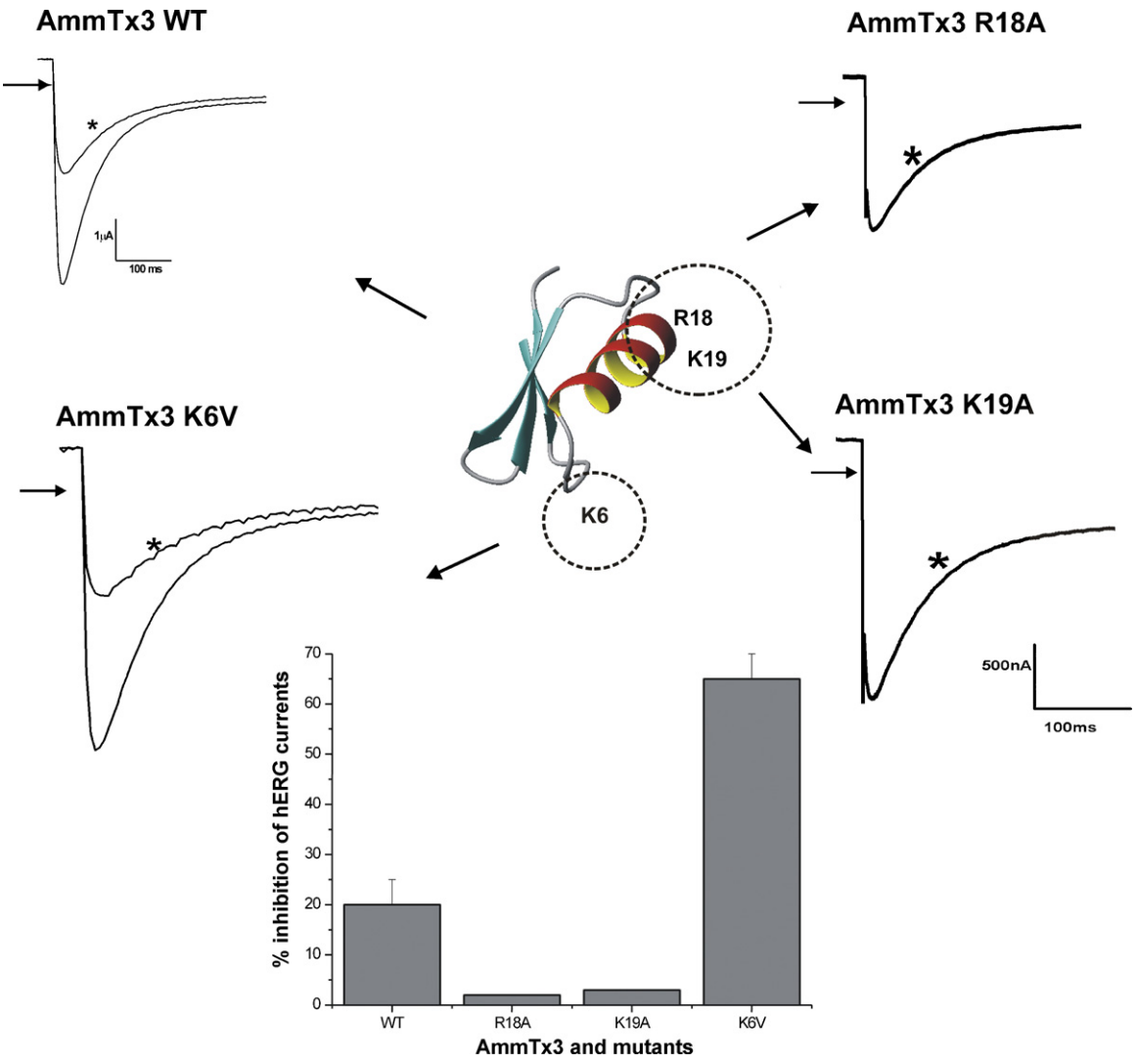

Fig. 4 – Selected traces showing the effect of AmmTx3 and its mutants on hERG channels. Two mutants where one basic residue involved in the pharmacophore has been replaced by alanine were constructed. The mutations abolished the hERG blocking activity at concentrations up to 3.5 μM ($n = 5$). Additionally, the IC_{50} value of AmmTx3K6V was very close to that of BmTx3 (3.2 ± 0.75 μM, $n = 8$). Statistical analysis between groups of data was carried out using the Student's *t*-test and a probability of <0.05 was considered to be statistically significant.

($n = 5$) respectively at a concentration of 2.4 μM. The discrepin double mutant failed to induce any effect, while the triple mutant could cause a block of hERG channels with an IC_{50} value of 3.5 ± 1 μM with $n = 5$. Additionally, a V6K mutant was constructed and tested and was found to have no effect on discrepin original inability to affect hERG channels (Fig. 5).

3.2.4. *Other α-KTx subfamilies*

Additionally, other toxins such as BmTx2, Tsκ, HsTx1 belonging to α-KTx1, α-KTx4 and α-KTx6 have been tested on hERG channels. Fig. 6 shows an alignment of the amino acid sequence of the selected toxins based on the cysteine residues. Interestingly, those toxins could induce a significant hERG block (Fig. 7) compared to the selected control group: PBTx3, TyKα and spinoxin, from the same α-KTx subfamilies.

4. Discussion

To date, a total of 28 hERG blockers from scorpion venom are known, 27 of which are grouped into γ-KTxs and only one, BmTx3, belongs to subfamily α-KTx15. The hERG blocking activity in BmTx3 has been assigned to a functional epitope formed of 2 basic residues R18 and K19 on the α-helix side of the peptide. Based on the model of BmTx3, we investigated the effect of other members of the same subfamily α-KTx15 starting with closest toxin to BmTx3 which is AmmTx3 (91% similarity, only 4 residues are different and only 1 case of charge addition V6K). AmmTx3 could induce a hERG channel block with no alteration of the gating kinetics. To assign the hERG blocking activity to the same "hot spot" as proposed in BmTx3, two single mutants have been made in AmmTx3: R18A and K19A which caused the loss of the hERG current inhibition

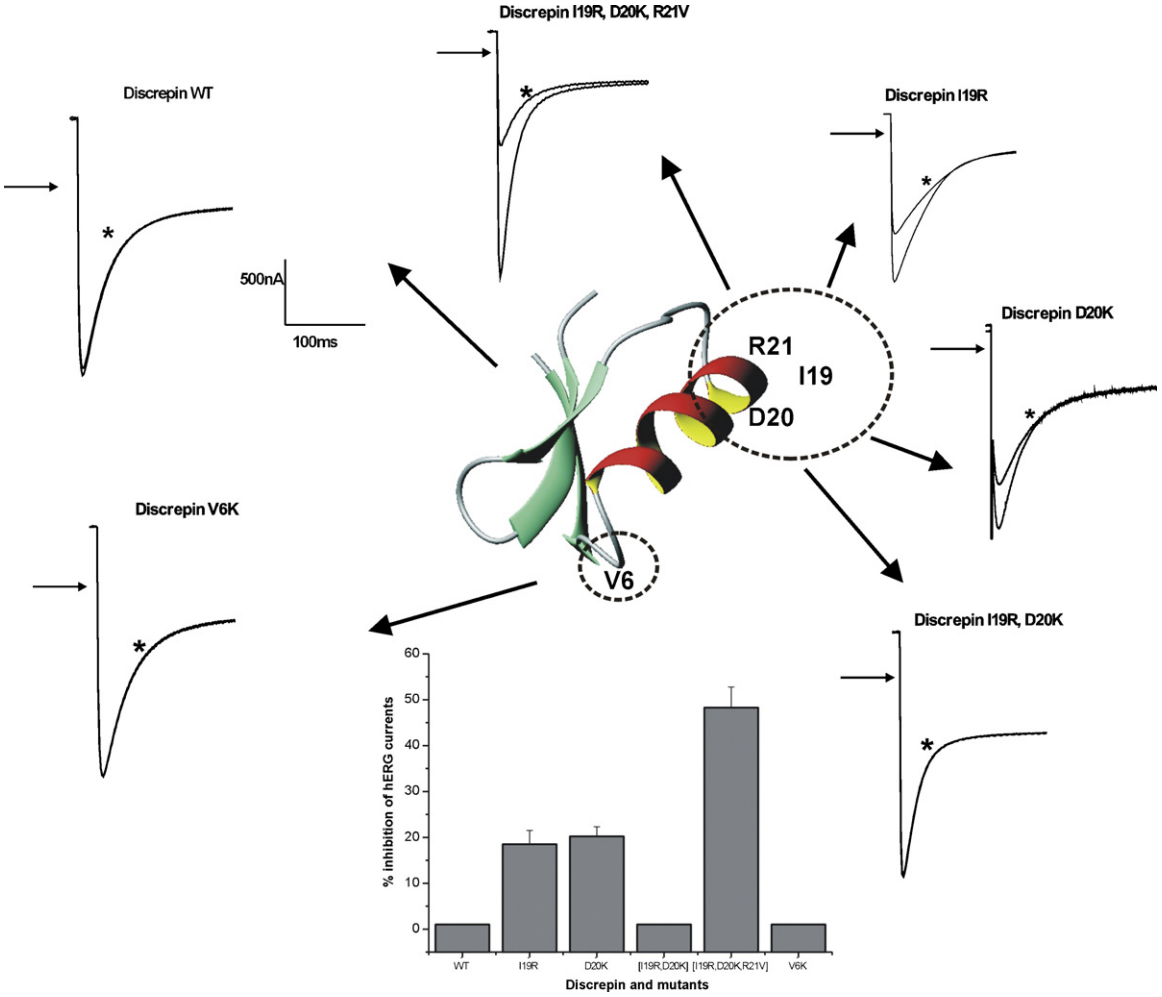

Fig. 5 – Selected traces showing the effects induced by discrepin and its mutants at a concentration of 3 μM. The discrepin mutants I19R and D20K could induce a block of 18.5 ± 3%, 20.2 ± 2.1% (n = 5) respectively. The discrepin double mutant failed to induce any effect, while the triple mutant could cause a block of hERG channels with an IC_{50} value of 3.5 ± 1 μM (n = 5). Finally, V6K mutant was found to have no effect on discrepin original inability to affect hERG channels.

```
                1         10        20        30
BmTx2     QFTNVSCSAS SQCWPVCKKL FGTYRGKCMN SKCRCYS.
PBTx3     -EVDMRCKSS KECLVKCKQA TGRPNGKCMN RKCKCYPR

Tsκ       VVIGQRCYRS PDCYSACKKL VGKATGKCTN GRCDC...
TyKα      VFINAKCRGS PECLPKCKEA IGKAAGKCMN GKCKCYP.

HsTx1     ----ASCRTP KDCADPCRKE TGCPYGKCMN RKCKCNRC
Spinoxin  ----IRCSGS RDCYSPCMKQ TGCPNAKCIN KSCKCYGC
```

Fig. 6 – Alignment of selected toxins of the α-KTx family which are able to block hERG channels based on the cysteine residues. The important residues involved in the proposed hERG epitope are highlighted in grey namely 2 positive residues a Lys or Arg after the 3rd cysteine. Each toxin bearing the hot spot is compared to a control toxin belonging to the same subfamilies of toxins and lacking the hot spot. The same programs and sources are used as in Fig. 2. Accession numbers: BmTx2: Q9NII5, PBTx3: P83112, Tsκ: P56219, Tyα: P46114, HsTx1: P59867, spinoxin: P84094.

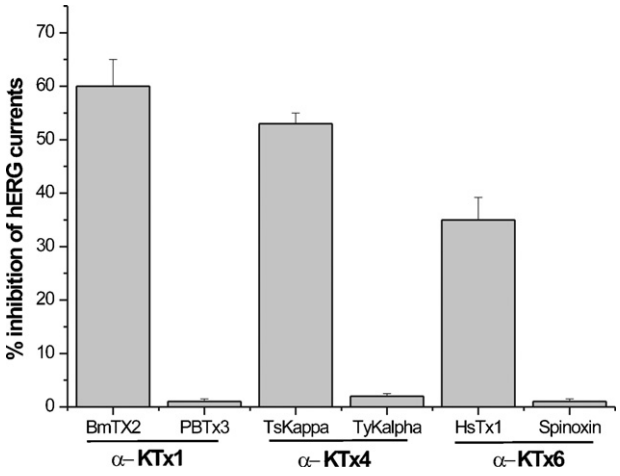

Fig. 7 – Overview of the effect of other α-KTx's possessing the double positive residues on hERG channels. BmTx2, Tsκ, HsTx1 which possess the "hot spot" have been tested on hERG channels at a concentration of 5 μM and have been found to inhibit hERG currents. The control group of toxins, i.e. PBTx3, TyKα and spinoxin had no effect at the same concentration.

ability. Moreover, we found that AmmTx3 was 4 fold less potent than BmTx3. The investigation of the sequence of AmmTx3 showed that position 6 of the toxin sequence is occupied by a positive residue Lys in contrast to BmTx3 which has a Val at the same position. Homology modeling generated a better view on the possible orientation of Lys at position 6 towards the proposed "hot spot" (Fig. 8) and the distance between Lys6 α-carbon and all the carbons of Arg18 was found to be 6.6 ± 0.1 Å on average. This orientation can lead to an extra positive cloud which might have an impact on the interaction between the epitope and the channel. This notion has been proven through a K6V point mutation where AmmTx3K6V showed an IC_{50} comparable to BmTx3.

To extend our theory to other members of subfamily α-KTx15, we tested the effects of a "hot spot"-bearing toxin and compared our results with a toxin without the "hot spot". The idea behind it was to see if hERG blocking activity could just be inherent of α-KTx15 subfamily. Therefore, we chose Aa1 (α-KTx 15.1 and possessing the "hot spot") which could induce a hERG channel block. Then we compared our results to discrepin (α-KTx15.6 and lacking the "hot spot") which did not affect hERG currents. Based on the above, we could assume that 2 basic residues located after the 3rd cysteine on the amino acid sequence of the toxins tested are responsible for the reduction of hERG currents independently of belonging to subfamily α-KTx15.

To consolidate our findings, and for the very first time, we constructed tailor-made toxins based on introducing hERG current inhibiting ability to the previously inactive discrepin. Our results show that the introduction of 1 positively charged residue either at position 19 or 20 can indeed introduce a hERG blocking activity to discrepin by forming the proposed pharmacophore making use of the native Arg at position 21. Interestingly, the introduction of 2 basic residues at the same time [I19R, D20K], completely abolished the toxin's ability to affect hERG channels presumably due to charge repulsion disfavouring the interaction between the toxin and the channel. Finally, replacing Arg21 by a Val was made to confirm that 3 adjacent positive residues in the double mutant are the reason for the loss of the effect and second, to check if the position of the pharmacophore was making a difference. From the results obtained, it appears that the position of the pharmacophore can either be **–CKKX-** or **–CKXK- or –CXKKX-**, with C being the 3rd cysteine and X being any non-positively charged amino acid and K being a Lys or Arg.

Other toxins such as BmTx2, Tsκ and HsTx1 are able to induce an inhibition of hERG currents at comparable concentrations to the tested toxins from α-KTx15 subfamily; hence, the extension of our model can be possible to other α-KTx subfamilies.

Since none of the toxins we tested caused alterations of the gating kinetics of hERG channels (Fig. 3), it seems reasonable to assume that α-KTxs are hERG pore blockers. The exact amino acids on the channel involved in the interaction with α-KTxs remain to be elucidated, ideally via co-crystallization, yet one can expect that the surface interaction can be comparable to that with BeKm-1 on which we based our model. Mutant cycle analysis earlier published by Tseng et al. [27], provides mechanistic insights into the unique features of BeKm-1/hERG interaction. The model constructed based on the analysis shows that BeKm-1 is stuck above the pore entrance by the S5-P1 and S5-P2 helices that crowd the outer vestibule of the channel. The S5-P helices make contacts with Tyr11 and Phe14 on one end of BeKm-1 α-helix. The other end of the toxin α-helix is pointing downward toward the pore entrance, with Lys18 and Arg20 making contacts with S631 side chains on two adjacent subunits. It is interesting to note that in this model, BeKm-1 is bound above the pore entrance and none of its side chains penetrate deep into the pore. This is distinctly different from the model of interaction of Charybdotoxin (ChTx) or AgTx2 binding to the Shaker channel, in which the critical Lys protrudes into the pore of the channel. Moreover, the model proposed by Tseng et al., indicates 4 important interaction amino acid residues (Tyr11, Phe14, Lys18 and Arg20) between BeKm-1 and hERG. However, for α-KTxs, only 2 interaction amino acid residues corresponding to Lys18 and Arg20 of BeKm-1 are proposed. Therefore, we can assume that α-KTxs possessing the "hot spot" are interacting only with the pore of hERG channels. A situation which can explain the relative lower potency of α-KTxs towards hERG channels compared with BeKm-1.

About half of the 120 α-KTx listed in 2004 by de la Vega et al. [13], have been tested directly against some K^+ channels and/or associated currents. For 59 of the peptides reported, there is no direct evidence of function described. The majority of the known functions have been determined on Shaker-related channels (subfamily Kv1.x) or on the Ca^{2+}-activated K^+ channels [13]. Therefore, our results provide new insight into the possible targets of α-KTxs. This could explain some of the intoxication symptoms caused by the venom and provide predictive tools for any new α-KTx to know the possible targets. It could also serve as predictive tool in drug design to either avoid or intentionally seek interaction with hERG channels. Furthermore, toxins that modulate hERG channels

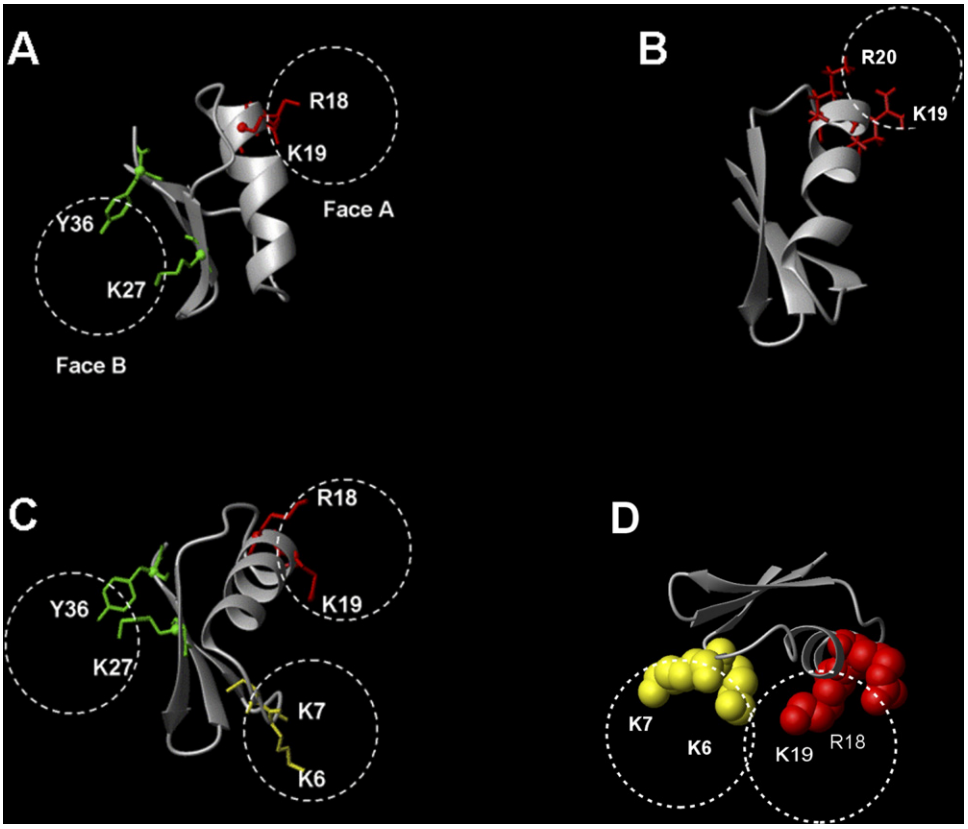

Fig. 8 – Model of AmmTx3 showing the 2 functional faces and the residues involved in the hERG-affecting epitope. *Panel A:* shows the model of the 2 faces of BmTx3 earlier published [1]. Face A is the proposed hERG "hot spot" formed of 2 positive residues R18 and K19 on the α-helix side of the peptide while face B contains the typical dyad formed of K27 and Y36. *Panel B:* shows a model of BeKm-1 with the important residues forming the epitope located on the α-helix. *Panel C, D:* a homology model of AmmTx3 showing the epitope located on the α-helix as well as K6 causing either steric hindrance or repulsion by the extra positive cloud in the space filling model. Homology models have been constructed using the first approach mode of SWISS-MODEL [47–49] and the results have been visualized in MOLMOL program [50].

are fundamental for the basic research aiming at understanding the molecular mechanisms of the channel, and hence, the development of new drugs to treat LQTS and Short QT syndrome (SQTS), muscular atrophy and many forms of cancer such as leukemia and uterus cancer which have also been associated with hERG channels [3].

Acknowledgements

We thank Prof. Keating M. for providing the cDNA for the hERG channels and Dr. Romi-lebrun R. for the synthesis of BmTx2 and HsTx1. The authors would like to acknowledge the skilful technical assistance of Ms Debaveye S. The authors would also like to thank Drs. Vandendriessche T., Dr. Diego-Garcia E. and Dr. Ricardo Rodriguez de la Vega for the constructive comments on the manuscript. This work was supported in part by grants OT/05-064, G.330.06 from the Fund for Scientific Research (FWO)-Flanders, P6/31 (Interuniversity attraction Poles Program- Belgian State- Belgian Science Policy) and DGAPA IN226006 (to G.C.) and IN227507 (to L.D.P.) from National Autonomous University of Mexico.

REFERENCES

[1] Huys I, Xu CQ, Wang CZ, Vacher H, Martin-Eauclaire MF, Chi CW, et al. BmTx3, a scorpion toxin with two putative functional faces separately active on A-type K^+ and HERG currents. Biochem J 2004;378:745–52.
[2] Sanguinetti MC, Jiang C, Curran ME, Keating MT. A mechanistic link between an inherited and an acquired cardiac arrhythmia: HERG encodes the IKr potassium channel. Cell 1995;81:299–307.
[3] Trudeau MC, Warmke JW, Ganetzky B, Robertson GA. HERG, a human inward rectifier in the voltage-gated potassium channel family. Science 1995;269:92–5.
[4] Curran ME, Splawski I, Timothy KW, Vincent GM, Green ED, Keating MT. A molecular basis for cardiac arrhythmia: HERG mutations cause long QT syndrome. Cell 1995;80:795–803.
[5] Vandenberg JI, Walker BD, Campbell TJ. HERG K^+ channels: friend and foe. Trends Pharmacol Sci 2001;22:240–6.
[6] Emmi A, Wenzel HJ, Schwartzkroin PA, Taglialatela M, Castaldo P, Bianchi L, et al. Do glia have heart? Expression and functional role for ether-a-go-go currents in hippocampal astrocytes. J Neurosci 2000;20:3915–25.

[7] Gullo F, Ales E, Rosati B, Lecchi M, Masi A, Guasti L, et al. ERG K^+ channel blockade enhances firing and epinephrine secretion in rat chromaffin cells: the missing link to LQT2-related sudden death? FASEB J 2003;17:330–2.
[8] Rosati B, Marchetti P, Crociani O, Lecchi M, Lupi R, Arcangeli A, et al. Glucose- and arginine-induced insulin secretion by human pancreatic beta-cells: the role of HERG K(+) channels in firing and release. FASEB J 2000;14:2601–10.
[9] Shoeb F, Malykhina AP, Akbarali HI. Cloning and functional characterization of the smooth muscle ether-a-go-go-related gene K^+ channel. Potential role of a conserved amino acid substitution in the S4 region. J Biol Chem 2003;278:2503–14.
[10] Smith GA, Tsui HW, Newell EW, Jiang X, Zhu XP, Tsui FW, et al. Functional up-regulation of HERG K^+ channels in neoplastic hematopoietic cells. J Biol Chem 2002;277: 18528–34.
[11] Hoffmann P, Warner B. Are hERG channel inhibition and QT interval prolongation all there is in drug-induced torsadogenesis? A review of emerging trends. J Pharmacol Toxicol Methods 2006;53:87–105.
[12] Tytgat J, Chandy KG, Garcia ML, Gutman GA, Martin-Eauclaire MF, van der Walt JJ, et al. A unified nomenclature for short-chain peptides isolated from scorpion venoms: alpha-KTx molecular subfamilies. Trends Pharmacol Sci 1999;20:444–7.
[13] Rodriguez de la Vega RC, Possani LD. Current views on scorpion toxins specific for K^+-channels. Toxicon 2004;43:865–75.
[14] Rodriguez de la Vega RC, Merino E, Becerril B, Possani LD. Novel interactions between K^+ channels and scorpion toxins. Trends Pharmacol Sci 2003;24:222–7.
[15] Dauplais M, Lecoq A, Song J, Cotton J, Jamin N, Gilquin B, et al. On the convergent evolution of animal toxins. Conservation of a diad of functional residues in potassium channel-blocking toxins with unrelated structures. J Biol Chem 1997;272:4302–9.
[16] M'Barek S, Mosbah A, Sandoz G, Fajloun Z, Olamendi-Portugal T, Rochat H, et al. Synthesis and characterization of Pi4, a scorpion toxin from Pandinus imperator that acts on K^+ channels. Eur J Biochem 2003;270:3583–92.
[17] Frenal K, Xu CQ, Wolff N, Wecker K, Gurrola GB, Zhu SY, et al. Exploring structural features of the interaction between the scorpion toxinCnErg1 and ERG K^+ channels. Proteins 2004;56:367–75.
[18] Lange A, Giller K, Hornig S, Martin-Eauclaire MF, Pongs O, Becker S, et al. Toxin-induced conformational changes in a potassium channel revealed by solid-state NMR. Nature 2006;440:959–62.
[19] Carbone E, Wanke E, Prestipino G, Possani LD, Maelicke A. Selective blockage of voltage-dependent K^+ channels by a novel scorpion toxin. Nature 1982;296:90–1.
[20] Miller C. The charybdotoxin family of K^+ channel-blocking peptides. Neuron 1995;15:5–10.
[21] Grissmer S, Nguyen AN, Aiyar J, Hanson DC, Mather RJ, Gutman GA, et al. Pharmacological characterization of five cloned voltage-gated K^+ channels, types Kv1.1, 1.2, 1.3, 1.5, and 3.1, stably expressed in mammalian cell lines. Mol Pharmacol 1994;45:1227–34.
[22] Zhang M, Liu XS, Diochot S, Lazdunski M, Tseng GN. APETx1 from sea anemone Anthopleura elegantissima is a gating modifier peptide toxin of the human ether-a-go-go-related potassium channel. Mol Pharmacol 2007;72: 259–68.
[23] Corona M, Gurrola GB, Merino E, Cassulini RR, Valdez-Cruz NA, Garcia B, et al. A large number of novel Ergtoxin-like genes and ERG K^+-channels blocking peptides from scorpions of the genus Centruroides. FEBS Lett 2002;532:121–6.
[24] Gurrola GB, Rosati B, Rocchetti M, Pimienta G, Zaza A, Arcangeli A, et al. A toxin to nervous, cardiac, and endocrine ERG K^+ channels isolated from Centruroides noxius scorpion venom. FASEB J 1999;13:953–62.
[25] Korolkova YV, Kozlov SA, Lipkin AV, Pluzhnikov KA, Hadley JK, Filippov AK, et al. An ERG channel inhibitor from the scorpion Buthus eupeus. J Biol Chem 2001;276: 9868–76.
[26] Nastainczyk W, Meves H, Watt DD. A short-chain peptide toxin isolated from Centruroides sculpturatus scorpion venom inhibits ether-a-go-go-related gene K(+) channels. Toxicon 2002;40:1053–8.
[27] Tseng GN, Sonawane KD, Korolkova YV, Zhang M, Liu J, Grishin EV, et al. Probing the outer mouth structure of the HERG channel with peptide toxin footprinting and molecular modelling. Biophys J 2007;92:3524–40.
[28] Korolkova YV, Bocharov EV, Angelo K, Maslennikov IV, Grinenko OV, Lipkin AV, et al. New binding site on common molecular scaffold provides HERG channel specificity of scorpion toxin BeKm-1. J Biol Chem 2002;277:43104–9.
[29] Vacher H, Alami M, Crest M, Possani LD, Bougis PE, Martin-Eauclaire MF. Expanding the scorpion toxin alpha-KTX 15 family with AmmTX3 from *Androctonus mauretanicus*. Eur J Biochem 2002;269:6037–41.
[30] Vacher H, Martin-Eauclaire MF. Antigenic polymorphism of the ''short'' scorpion toxins able to block K^+ channels. Toxicon 2004;43:447–53.
[31] Vacher H, Prestipino G, Crest M, Martin-Eauclaire MF. Definition of the alpha-KTx15 subfamily. Toxicon 2004;43:887–94.
[32] Legros C, Bougis PE, Martin-Eauclaire MF. Characterisation of the genes encoding Aa1 isoforms from the scorpion *Androctonus australis*. Toxicon 2003;41:115–9.
[33] D'Suze G, Batista CV, Frau A, Murgia AR, Zamudio FZ, Sevcik C, et al. Discrepin, a new peptide of the sub-family alpha-ktx15, isolated from the scorpion *Tityus discrepans* irreversibly blocks K^+-channels (IA currents) of cerebellum granular cells. Arch Biochem Biophys 2004;430:256–63.
[34] Prochnicka-Chalufour A, Corzo G, Satake H, Martin-Eauclaire MF, Murgia AR, Prestipino G, et al. Solution structure of discrepin, a new K^+-channel blocking peptide from the alpha-KTx15 subfamily. Biochemistry 2006;45:1795–804.
[35] Roche O, Trube G, Zuegge J, Pflimlin P, Alanine A, Schneider G. A virtual screening method for prediction of the HERG potassium channel liability of compound libraries. Chembiochem 2002;3:455–9.
[36] Lowenadler B, Jansson B, Paleus S, Holmgren E, Nilsson B, Moks T, et al. A gene fusion system for generating antibodies against short peptides. Gene 1987;58:87–97.
[37] Wei D, Li M, Zhang X, Xing L. An improvement of the site-directed mutagenesis method by combination of megaprimer, one-side PCR and DpnI treatment. Anal Biochem 2004;331:401–3.
[38] Drevet P, Lemaire C, Gasparini S, Zinn-Justin S, Lajeunesse E, Ducancel F, et al. High-level production and isotope labeling of snake neurotoxins, disulfide-rich proteins. Protein Exp Purif 1997;10:293–300.
[39] Park CS, Hausdorff SF, Miller C. Design, synthesis, and functional expression of a gene for charybdotoxin, a peptide blocker of K^+ channels. Proc Natl Acad Sci USA 1991;88:2046–50.
[40] Corzo G, Escoubas P, Villegas E, Karbat I, Gordon D, Gurevitz M, et al. A spider toxin that induces a typical effect of scorpion alpha-toxins but competes with beta-toxins on binding to insect sodium channels. Biochemistry 2005;44:1542–9.
[41] Sonnichsen FD, Van Eyk JE, Hodges RS, Sykes BD. Effect of trifluoroethanol on protein secondary structure: an NMR

and CD study using a synthetic actin peptide. Biochemistry 1992;31:8790–8.
[42] Corzo G, Escoubas P, Villegas E, Barnham KJ, He W, Norton RS, et al. Characterization of unique amphipathic antimicrobial peptides from venom of the scorpion Pandinus imperator. Biochem J 2001;359: 35–45.
[43] Romeo S, Corzo G, Vasile A, Satake H, Prestipino G, Possani LD. A positive charge at the N-terminal segment of Discrepin increases the blocking effect of K(+) channels responsible for the I(A) currents in cerebellum granular cells. Biochim Biophys Acta 2008.
[44] Vita C, Roumestand C, Toma F, Menez A. Scorpion toxins as natural scaffolds for protein engineering. Proc Natl Acad Sci USA 1995;92:6404–8.
[45] Wang I, Wu SH, Chang HK, Shieh RC, Yu HM, Chen C. Solution structure of a K(+)-channel blocker from the scorpion *Tityus cambridgei*. Protein Sci 2002;11: 390–400.
[46] Hall TA. BioEdit: a user-friendly biological sequence alignment editor and analysis program for Windows 95/98/ NT. Nucl Acids Symp Ser 1999;41:95–8.
[47] Arnold K, Bordoli L, Kopp J, Schwede T. The SWISS-MODEL workspace: a web-based environment for protein structure homology modelling. Bioinformatics 2006;22:195–201.
[48] Kopp J, Schwede T. Automated protein structure homology modeling: a progress report. Pharmacogenomics 2004;5:405–16.
[49] Kopp J, Schwede T. The SWISS-MODEL Repository of annotated three-dimensional protein structure homology models. Nucleic Acids Res 2004;32:D230–4.
[50] Koradi R, Billeter M, Wuthrich K. MOLMOL: a program for display and analysis of macromolecular structures. J Mol Graph 1996;14(51-5):29–32.